Journal of Oil Palm Research Vol. 34 (1) March 2022 p. 35-45
DOI: https://doi.org/10.21894/jopr.2021.0021

HISTONE MODIFICATION MARKS IMPROVE IDENTIFICATION OF OIL PALM TRANSCRIPTION START SITES

SARPAN, N[1]; TATARINOVA, T V[2]; LOW, E-T L[1]; ONG-ABDULLAH, M[1]; SAPIAN, I S[3] and OOI, S-E[1]*

ABSTRACT

Epigenetic regulation involves modifications of chromatin components such as post-translational modifications of histone proteins, methylation of cytosines in deoxyribonucleic acid (DNA), the involvement of small RNA and chromatin remodeling. Numerous methods have been established to understand the epigenetic control of agronomically important traits. Chromatin immunoprecipitation with sequencing (ChIP-Seq) is widely used to identify the binding sites of transcription factors or modified histones on a genome-wide scale. Here, ChIP-Seq targeting H3K4me3 and H3K27me3 marks in oil palm spears were conducted to examine genomic regions enriched with these histone modifications. Due to low DNA amounts from ChIP experiments, the data analysis workflow was optimised based on ChIP-Seq workflows on other plants. Mapping to specific target regions revealed that the histone mark peak positions were located close to predicted transcription start sites (TSS). This agrees with H3K4me3 and H3K27me3 profiles in other plants where H3K4me3 marks are generally associated with active genes and promoter regions while H3K27me3 marks are linked to repressed genes. Gene-wide mapping for low coverage ChIP-Seq data showed that H3K4me3 and H3K27me3 profiles on the oil palm genome corresponded to consensus histone profiles in other plants. This is the first ChIP-Seq analysis workflow reported for oil palm spears, which can be used to develop future oil palm ChIP-Seq studies.

Keywords: ChIP-Seq, *Elaeis guineensis*, epigenetics, H3K4me3, H3K27me3.

Received: 19 October 2020**; Accepted:** 2 February 2021**; Published online:** 19 May 2021.

INTRODUCTION

Epigenetics mechanisms lead to spatial-temporal gene expression changes that are not mediated by changes in the underlying deoxyribonucleic acid (DNA) sequence (Wollmann and Berger, 2012). Unlike the genome, the epigenome is dynamically altered by environmental factors (Baulcombe and Dean, 2014). In oil palm, crop improvement programmes involve numerous breeding trials, which are then selected for massive multiplication through tissue culture (Zulkifli *et al.*, 2017). However, the production of elite clonal materials has yet to be maximised due to the occurrence of mantled fruits that causes oil and yield losses. Through epigenome-wide association studies, the loss of DNA methylation at the E*gDEF1*'s *Karma* epi-allele in tissue culture regenerants was associated with the mantling phenotype (Ong-Abdullah *et al.*, 2015). Subsequently, an epi-fingerprinting assay for *in vitro* cultured palms was developed to discriminate true-to-types from off-types (Ong-Abdullah *et al.*, 2016). This step serves as quality control (QC) to improve the efficiency of the tissue culture process and thus, marks the beginning of applied epigenetics for the

[1] Malaysian Palm Oil Board,
6 Persiaran Institusi, Bandar Baru Bangi,
43000 Kajang, Selangor, Malaysia.

[2] Department of Biology, University of La Verne,
La Verne CA, USA.

[3] Malaysian Genome Institute,
National Institute of Biotechnology Malaysia,
Jalan Bangi, 43000 Kajang, Selangor, Malaysia.

* *Corresponding author e-mail: oseng@mpob.gov.my*

oil palm industry through the identification of low-risk planting materials.

Chromatin, which is built by a nucleosome array containing 147 bp of DNA and pairs of histones H2A, H2B, H3 and H4, acts as a target for epigenetic modifiers comprising methylation of cytosines in the DNA, modifications at the N-terminal tails of histone proteins and small non-coding ribonucleic acid (RNA) molecules (Lu *et al.*, 2020). These mechanisms affect the packaging of chromatin and accessibility of the transcriptional machinery, thus, influencing gene expression. The pattern of modifications on histone tails, known as the histone code, contribute to shaping chromatin structure into either condensed heterochromatin or open euchromatin (Prakash and Fournier, 2018). H3K4me3 and H3K27me3 are two widely investigated histone marks in plants. The wide distribution of H3K4me3 marks in promoter regions is associated with active transcription, while H3K27me3 marks are usually associated with the Polycomb Repressive Complex involved in gene silencing (Gan *et al.*, 2015; Zhang *et al.*, 2009). In plants, histone modification signatures are seen for several developmental processes, including response to stress (Zeng *et al.*, 2019), flower morphogenesis (Engelhorn *et al.*, 2017) and embryogenesis (Berenguer *et al.*, 2017). Studies on histone modifications often involve locating their binding sites through a method called chromatin immunoprecipitation with sequencing (ChIP-Seq) (Liu *et al.*, 2010). In ChIP-Seq, genomic DNA is first fragmented, followed by the capturing of histone-bound fragments. The non-histone fractions are then discarded, leaving only the enriched fraction that will be sequenced. Subsequent bioinformatics analysis of ChIP-Seq datasets generally includes QC checks of sequencing reads, aligning reads to the reference genome and finding peaks corresponding to ChIP-enriched regions. Reported ChIP-Seq data usually involves at least 20 million mapped reads (Zhang *et al.*, 2015; Zong *et al.*, 2013), but the chromatin immunoprecipitation step generally provides low yields in the nanogram range (Ranawaka *et al.*, 2020). Thus, reads duplication is more apparent when insufficient DNA from inefficient immunoprecipitation is used in constructing sequencing library and becomes more abundant when the library is deeply sequenced (Landt *et al.*, 2012).

In this study, the histone modifications H3K4me3 and H3K27me3 in oil palm leaf spear tissue were investigated using ChIP-Seq. These two histone modifications were selected based on their influence on transcriptional regulation, whereby the H3K4me3 is associated with active transcription while the H3K27me3 is linked to repressed transcription at gene-rich regions. The DNA bound to histones enriched with these two histone modifications was immunoprecipitated and sequenced. The low DNA yields obtained through ChIP led to low coverage ChIP-Seq data. To circumvent this limitation and still gain preliminary insights on these histone marks in oil palm, a gene-wide mapping approach was able to demonstrate that H3K4me3 and H3K27me3 profiles in oil palm are in concordance with their consensus distribution patterns on gene regions in other plants. To our knowledge, this is the first report of a ChIP-Seq workflow described for the oil palm.

MATERIALS AND METHODS

Plant Material

Spear leaf tissues of 10 clonal palms at the MPOB Bagan Datuk Research Station, Perak, Malaysia were sampled, frozen in liquid nitrogen and stored at -80°C until further use. The palms, labeled from A to J (*Table 1*), originated from the same tissue used in *in vitro* cloning and are thus, grouped as biological replicates.

Chromatin Immunoprecipitation and Sequencing

Chromatin was isolated following a protocol described by Kaufmann *et al.* (2010), with modifications, as described by Sarpan *et al.* (2018). Briefly, the spears were ground in liquid nitrogen, added with lysis buffer and cold-incubated. The mixture was filtered and centrifuged to collect the pellet. The pellet underwent a few series of washing steps prior to shearing. Chromatin was sheared using a Covaris M220 (Covaris, USA) for 25 min in a screw-cap microtube at 4°C with the following settings: 5% duty factor and 200 cycles/burst. ChIP-validated antibodies, anti-H3K4me3 (ab12209) and anti-H3K27me3 (ab6002, Abcam, United Kingdom), as used by Sarpan *et al.* (2018) and EpiSeeker ChIP Kit-Plants (Abcam, United Kingdom) were used for immunoprecipitation in this study. Sequencing libraries were prepared from ChIP DNA using the TruSeq® ChIP library preparation kit (Illumina, USA). The amount of input DNA (non-immunoprecipitated) used was 10 ng, while ChIP DNA starting amounts were varied between 1 and 5 ng. A total of 10 H3K27me3 ChIP-Seq libraries were prepared but only nine H3K4me3 ChIP-Seq libraries were generated as library preparation failed for one of the samples. Libraries were sequenced paired-end at a read-length of 125 bp on a HiSeq2500 Illumina platform with a depth of at least 20 million reads.

ChIP-Seq Analysis

The quality of sequencing reads was assessed using FastQC v0.11.3 software (Babraham Bioinformatics). Raw reads were trimmed using Flexbar v3.4.0 (Dodt *et al.*, 2012) to filter out

TABLE 1. ChIP-SEQ DATASETS MAPPED TO GENOME-WIDE

Histone modification	Library type	Biological replicate	Raw reads	[a]Trimmed reads	[b]Mapped reads	[c]Non-duplicate reads	[d]Total bases (all positions)	Bases with 0 read	Bases with ≥1 reads	[e]Genome coverage (%)	[f]Read coverage per base
H3K4me3	control	A	35 984 910	35 669 154	35 435 466	27 736 510	1 533 938 362	724 607 480	809 330 882	52.76	4.15
		B	52 050 286	51 645 526	51 260 135	44 625 812	1 534 342 085	586 712 882	947 629 203	61.76	5.71
		C	44 381 902	43 997 588	43 663 651	29 644 138	1 534 144 289	683 468 435	850 675 854	55.45	4.22
		D	51 083 054	50 730 270	50 409 026	26 731 614	1 533 860 846	813 524 274	720 336 572	46.96	4.46
		E	42 168 806	41 837 986	41 552 394	29 891 260	1 534 001 008	712 662 441	821 338 567	53.54	4.40
		G	31 800 882	31 520 392	31 273 417	22 813 368	1 534 001 840	745 401 962	788 599 878	51.41	3.51
		H	43 756 708	43 306 396	42 991 826	41 011 330	1 534 132 957	580 113 958	954 018 999	62.19	5.23
		I	45 063 152	44 692 636	44 387 622	33 418 384	1 533 094 523	839 258 804	693 835 719	45.26	5.81
		J	36 742 346	36 400 994	36 126 280	34 781 924	1 534 176 063	624 238 482	909 937 581	59.31	4.65
H3K4me3	ChIP	A	75 862 582	74 810 274	74 233 306	12 315 882	1 533 453 476	974 321 640	559 131 836	36.46	2.66
		B	197 624 588	195 934 548	194 325 596	30 171 318	1 534 277 620	707 660 415	826 617 205	53.88	4.39
		C	31 412 106	31 142 214	30 666 435	5 612 798	1 530 823 722	1 205 596 031	325 227 691	21.25	2.08
		D	41 919 552	41 336 506	40 039 231	1 144 332	1 500 495 388	1 424 719 833	75 775 555	5.05	1.77
		E	37 965 452	37 673 322	37 148 105	4 575 718	1 529 556 467	1 265 983 936	263 572 531	17.23	2.08
		G	30 519 894	30 095 468	29 652 732	888 572	1 492 505 662	1 427 678 548	64 827 114	4.34	1.61
		H	39 010 174	38 420 070	37 793 093	1 972 456	1 514 677 266	1 382 847 468	131 829 798	8.70	1.77
		I	41 431 160	41 078 370	40 688 442	12 273 908	1 533 401 893	945 981 023	587 420 870	38.31	2.53
		J	31 687 056	31 418 340	29 694 600	2 759 248	1 522 564 714	1 346 184 740	176 379 974	11.58	1.87
H3K27me3	control	A	42 210 292	41 827 008	41 538 453	39 473 908	1 534 224 788	614 003 122	920 221 666	59.98	5.22
		B	46 295 636	45 851 060	45 506 248	43 114 494	1 534 212 412	578 584 051	955 628 361	62.29	5.49
		C	45 928 412	45 554 732	45 207 704	42 536 726	1 534 283 404	581 509 659	952 773 745	62.10	5.43
		D	38 714 154	38 364 604	38 108 722	36 248 822	1 534 182 116	635 612 490	898 569 626	58.57	4.91
		E	43 061 204	42 605 744	42 319 874	39 330 794	1 534 193 919	604 591 944	929 601 975	60.59	5.14
		F	43 003 696	42 602 988	42 314 438	36 935 124	1 534 202 778	613 186 747	921 016 031	60.03	4.88
		G	44 338 502	43 910 016	43 597 559	41 560 574	1 534 240 271	589 113 789	945 126 482	61.60	5.35
		H	42 273 554	42 001 334	41 707 342	31 618 422	1 534 196 992	655 137 242	879 059 750	57.30	4.37
		I	38 556 918	38 204 874	37 945 426	35 059 998	1 534 159 267	629 116 433	905 042 834	58.99	4.72
		J	43 319 140	42 897 120	42 608 417	38 481 480	1 534 100 471	591 154 107	942 946 364	61.47	4.96

TABLE 1. ChIP-SEQ DATASETS MAPPED TO GENOME-WIDE (continued)

Histone modification	Library type	Biological replicate	Raw reads	[a]Trimmed reads	[b]Mapped reads	[c]Non-duplicate reads	[d]Total bases (all positions)	Bases with 0 read	Bases with ≥1 reads	[e]Genome coverage (%)	[f]Read coverage per base
H3K27me3	ChIP	A	39 351 328	38 796 698	35 957 556	1 238 748	1 502 697 938	1 418 341 444	84 356 494	5.61	1.72
		B	34 223 168	33 686 222	32 394 786	3 189 744	1 524 866 923	1 318 306 613	206 560 310	13.55	1.85
		C	32 242 982	31 992 096	31 521 609	6 887 100	1 531 912 824	1 133 843 209	398 069 615	25.99	2.09
		D	40 658 292	40 110 788	35 257 532	6 727 856	1 532 091 408	1 166 333 508	365 757 900	23.87	2.22
		E	47 270 818	46 593 894	44 711 067	1 394 144	1 505 655 829	1 413 482 364	92 173 465	6.12	1.79
		F	46 424 912	45 977 946	45 627 608	35 221 778	1 534 212 270	608 918 890	925 293 380	60.31	4.63
		G	21 385 898	21 071 740	20 673 777	917 326	1 495 112 267	1 425 848 085	69 264 182	4.63	1.57
		H	34 458 854	34 167 082	33 471 587	5 316 020	1 530 673 976	1 207 494 470	323 179 506	21.11	1.98
		I	36 855 828	36 572 002	36 136 392	6 325 896	1 531 558 077	1 193 266 507	338 291 570	22.09	2.26
		J	35 552 140	35 069 174	34 490 720	3 386 116	1 525 684 917	1 309 144 878	216 540 039	14.19	1.88

Note: [a]Total reads after trimming using Flexbar.
[b]Total reads after mapping using Bowtie2.
[c]Total reads after duplicates removal using samtools markdup function in SAMtools package.
[d]Total bases (positions) identified using samtools depth function in SAMtools package.
[e]Percentage of genome covered with ChIP-Seq reads.
[f]Average number of reads at any position in the genome.

contaminated adapter sequences and low-quality reads. The trimmed reads were aligned to (1) *Elaeis guineensis* P5-build reference genome (NCBI BioProject accessions PRJNA192219, accessions ASJS00000000) (Singh *et al.*, 2013) and, (2) gene models (Sanusi *et al.*, 2018) ±1 kb flanking regions (define as 'gene-wide'), using Bowtie2 v2.2.5 (Langmead and Salzberg, 2012) with --very-sensitive-local settings. Removal of duplicate reads and read coverage assessments were performed using SAMtools v1.9 (Li *et al.*, 2009). Mean coverage was calculated in R. Histone-bound regions were identified using MACS2 v2.1.1.20160309 (Zhang *et al.*, 2008) with options *-q* 0.05 specified for H3K4me3, while *--broad --broad-cutoff* 0.05 was conducted for H3K27me3. Gene-wide distribution patterns of pooled H3K4me3 and H3K27me3 peaks was plotted based on the average pileup reads of the peaks calculated for a 2 kb window around gene translation start positions and visualised using R. Average pileup is calculated by adding the pileup for individual genes at all positions of the detected peak and then dividing by the number of peaks. Prediction of TSS was made using SoftBerry tools. ChIP-Seq data can be accessed under GEO Accession No. GSE159142.

RESULTS

Raw sequencing reads in *fastq* format was analysed with FastQC, which provides a quality assessment of the raw sequencing data. For all datasets, quality scores per base were generally good with a slight decrease towards the end of the reads. Approximately 1%-2% of the sequence reads were eventually discarded during the read trimming process due to the presence of adapter sequences and low-quality calls (*Table 1*).

Low ChIP Recovery for ChIP-Seq Lead to Low Sequence Coverage and High Duplication

In standard bioinformatics pipelines, sequencing reads are made informative by mapping to a reference genome using an aligner software. In this study, the trimmed reads were initially aligned to the P5-build of the *E. guineensis* reference genome (Singh *et al.*, 2013). This step generated an alignment result in the Sequence Alignment/Map (SAM) format, which assigns specific genomic locations to each read. H3K4me3 and H3K27me3 ChIP-Seq sets in this study comprised the ChIP and their respective non-immunoprecipitated (denoted hereafter as control) sequencing data. While biological replicates A-J in the control group showed a consistent mapping percentage of more than 99%, mapping efficiencies of the immunoprecipitated biological replicates A-J were lower, ranging from 95%-99% for H3K4me3 and 88%-99% for H3K27me3 (*Table 2*). The

overall read mapping performance was acceptable (*Figure 1*), but duplication was high in each ChIP data compared to their corresponding control (*Figure 2* and *Table 2*). The high amount of duplicates was probably due to the low amounts of ChIP DNA used to prepare the ChIP-Seq libraries. Duplicates also reflect the redundant reads resulting from polymerase chain reaction (PCR) overamplification, leading to an over-representation of ChIP-Seq reads at some genomic regions (Loh *et al.*, 2017). The duplicates are technically identified as read pairs with their 5′ ends mapped to the same genomic coordinates. Removal of duplicates was deemed necessary in this study due to the high duplication observed; otherwise peak calling or statistical analyses would be affected by the high duplication. Removal of duplicates thus, led to significant losses in reads, leaving only <20% of data for further analysis (*Figure 2*). The number of remaining reads after duplicates removal did not correlate with the amounts of starting material used to prepare the ChIP-Seq libraries (*Tables 1* and *2*). While control data mapped to 45%-62% of the genome, only 4%-60% of the genome was covered by ChIP reads (*Table 1*). On average, about 4-6 mapped reads per base were observed in control data, but only 2-4 and 2-5 read coverage was observed for H3K4me3- and H3K27me3-ChIP data respectively (*Table 1*). Overall, the immunoprecipitated ChIP-Seq data had high duplication rates and reduced coverage, which was most likely due to the low starting DNA input for library preparation, and is therefore not suitable for genome-wide analysis. However, it may still be useful for a targeted working hypothesis limited to selective regions, *e.g.*, genes, repeats and intergenic regions, as reported in the following section.

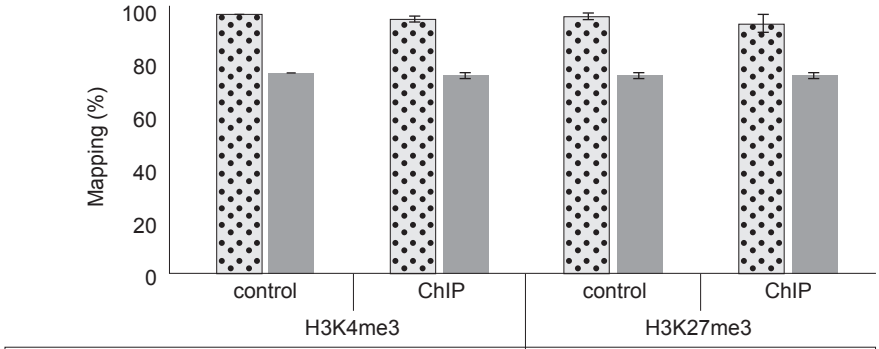

genome-wide	99.29	98.09	99.30	96.37
gene-wide	76.47	75.84	75.80	74.49

Figure 1. Average mapping percentages of ChIP-Seq data aligned to genome-wide and gene-wide E. guineensis pisifera *reference databases. Error bars indicate standard deviation (H3K4me3; n=9 and H3K27me3; n=10). Values below indicate the mapping percentage of each bar.*

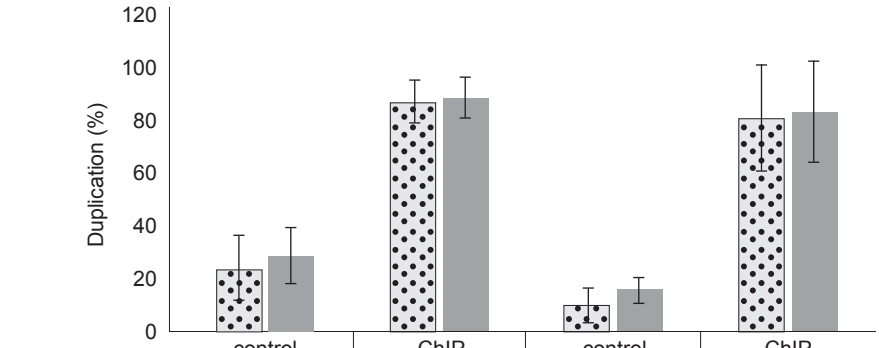

genome-wide	22.99	87.61	9.30	82.26
gene-wide	27.30	89.17	14.89	83.81

Figure 2. Presence of sequence duplicates in ChIP-Seq data aligned to genome-wide or gene-wide E. guineensis pisifera *reference databases. Error bars indicate standard deviation (H3K4me3; n=9 and H3K27me3; n=10). Values below indicate the percentage of duplication for each bar.*

TABLE 2. SUMMARY OF ChIP-SEQ DATASETS

Histone modification	Library type	Biological replicate	[a]Library starting material	[b]Mapping (%)		[c]Duplication (%)	
				Genome-wide	Gene-wide	Genome-wide	Gene-wide
H3K4me3	control	A	10	99.34	76.49	22.24	25.68
		B	10	99.25	75.76	13.59	18.30
		C	10	99.24	76.09	32.62	35.55
		D	10	99.37	77.03	47.31	50.59
		E	10	99.32	76.51	28.55	31.80
		G	10	99.22	76.21	27.62	30.39
		H	10	99.27	76.07	5.30	11.09
		I	10	99.32	78.40	25.23	32.84
		J	10	99.25	75.64	4.45	9.50
H3K4me3	ChIP	A	5.79	99.23	76.43	83.54	85.58
		B	2.10	99.18	77.12	84.60	87.28
		C	1.43	98.47	76.30	81.98	83.85
		D	3.81	96.86	74.65	97.23	97.79
		E	5.38	98.61	75.96	87.85	89.57
		G	4.01	98.53	76.21	97.05	97.70
		H	2.23	98.37	76.59	94.87	95.84
		I	7.29	99.05	76.50	70.12	72.60
		J	6.21	94.51	72.84	91.22	92.31
H3K27me3	control	A	10	99.31	75.48	5.63	12.00
		B	10	99.25	75.72	5.97	12.73
		C	10	99.24	75.70	6.63	12.14
		D	10	99.33	75.63	5.51	11.73
		E	10	99.33	75.93	7.69	12.94
		F	10	99.32	75.96	13.30	18.51
		G	10	99.29	75.78	5.35	11.77
		H	10	99.30	76.12	24.72	28.78
		I	10	99.32	75.75	8.23	13.25
		J	10	99.33	75.96	10.29	15.08
H3K27me3	ChIP	A	2.38	92.68	71.76	96.81	97.25
		B	2.68	96.17	74.07	90.53	91.74
		C	3.70	98.53	75.95	78.47	80.47
		D	2.71	87.90	67.79	83.23	83.25
		E	4.74	95.96	73.88	97.01	97.65
		F	10.10	99.24	76.32	23.39	28.48
		G	2.95	98.11	76.41	95.65	96.40
		H	1.12	97.96	75.93	84.44	86.19
		I	4.35	98.81	76.51	82.70	84.90
		J	3.81	98.35	76.25	90.34	91.79

Note: [a]DNA recovered from immunoprecipitation reactions used to prepare ChIP-Seq library.
[b]Percentage of reads mapped to the reference databases using Bowtie2.
[c]Duplicates presence in the mapped reads.

Gene-wide as an Alternative to Genome-wide Alignment

Read mapping on a genome-wide scale is a common practice in next-generation sequencing analysis and is widely acknowledged as a reliable approach when biases and limitations are minimal. With the limited number of unique ChIP reads, an alternative is to map onto a targeted region. In this study, a gene-wide database was built from genic areas consisting of gene models from their translation start to stop ±1 kb of their flanking upstream and downstream regions. The upstream 1 kb region would contain part of the promoter regions important for gene regulation, including the transcription start sites located around 50-200 bp upstream of the start codon (Shahmuradov *et al.*, 2017). These genic, upstream and downstream regulatory regions are usually covered by H3K4me3 and H3K27me3 modifications in other plants such as *Arabidopsis*, peach and potato (de la Fuente *et al.*, 2015; Yang *et al.*, 2018; Zeng *et al.*, 2019). This database generated for the oil palm was ~236 Mb, comprising 24 927 genes with their upstream and downstream regions. Predicted TSS are available for 13 016 genes. As a small portion of genes have multiple predicted TSS, a total of 14 353 TSS and 16 405 transcription termination sites (TTS) positions were identified. Gene-wide mapping rates were only slightly lower compared to genome-wide (*Figure 1*), with the majority of reads in ChIP and control datasets (~75%) mapping to genic regions (*Table 2*). The remaining 25%, therefore, most likely mapped to intergenic regions. This observation also suggested that most H3K4me3 and H3K27me3 marks are focused on or near genic regions. These observations are in agreement with the properties of H3K4me3 and H3K27me3 marks reported for plants such as *Arabidopsis*, peach and potato (de la Fuente *et al.*, 2015; Yang *et al.*, 2018; Zeng *et al.*, 2019), *i.e.*, both marks are highly associated with regulatory elements of genes and transcription. These results also suggested that the low coverage ChIP-Seq data could provide preliminary insights into H3K4me3 and H3K27me3 profiles on targeted oil palm genic regions. The current version of the oil palm genome assembly is a preliminary one (Chan *et al.*, 2017); there are 40 360 genomic scaffolds, ranging in length from 1992 to 22 100 610 nt. By focusing on the relevant regions (genic and regulatory) of well-annotated genes, we avoid 'dilution' of the signal from spurious mapping of reads to incorrectly assembled regions. This approach has improved the mapping precision of ChIP-Seq reads on target genic regions. However, the ChIP method on oil palm spears will require further optimisation to increase the DNA yield recovery, most likely by pooling an increased number of immunoprecipitation reactions.

Histone Marks Highly Associate with Predicted TSS of Genes

After mapping analysis, genomic regions with ChIP enrichment over background noise were detected as peaks using the Model-based Analysis of ChIP-Seq (MACS2) peak-calling software. These 'called peaks' represent biologically relevant histone modification sites. Peak detection parameters were optimised based on the binding properties of the specific histone modification, *i.e.*, a 'sharp' feature for H3K4me3 and a 'broad' feature for H3K27me3 at 0.05 false discovery rate (FDR) cut-off. Using the MACS2 peak caller, 300 to 4000 peaks associating with H3K4me3 and H3K27me3 were identified, albeit inconsistently among the biological replicates, likely due to their low coverage (*Table 3*). The H3K4me3 and H3K27me3 peak distribution profiles indicated that their abundance was predominant near the predicted TSS of genes (*Figure 3*). The oil palm H3K4me3 profile showed a narrow distribution with its peak centered at the predicted TSS (located on average 100 bp upstream of translation start positions) (*Figure 3a*), while H3K27me3 peak profile was much broader and was distributed over the gene region from the TSS (*Figure 3b*). These profiles were generally consistent with H3K4me3 and H3K27me3 patterns in other plants (de la Fuente *et al.*, 2015; Yang *et al.*, 2018; Zeng *et al.*, 2019). These profiles suggest that low coverage ChIP-Seq data could still reveal prominent characteristics of these histone modification profiles in oil palm.

TABLE 3. NUMBER OF ChIP-SEQ PEAKS IDENTIFIED USING MACS2 PACKAGE

Histone modification	Biological replicate	No. of ChIP-Seq peaks
H3K4me3	A	2 235
	B	3 623
	C	504
	D	743
	E	1 584
	G	296
	H	1 168
	I	3 910
	J	580
H3K27me3	A	739
	B	707
	C	1 227
	D	1 436
	E	727
	F	1 581
	G	472
	H	762
	I	1 348
	J	918

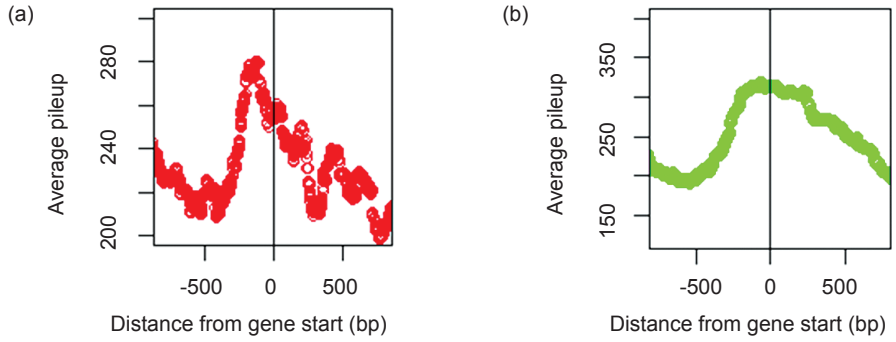

Figure 3. Gene-wide distribution pattern of ChIP-Seq peaks near the transcription start sites. (a) narrow distribution of H3K4me3 profile; (b) broad distribution of H3K27me3 profile. '0' on the x-axis denotes the ATG start codon.

DISCUSSION

In this study, H3K4me3 and H3K27me3 ChIP-Seq libraries were prepared with low amounts of DNA from pooled ChIP reactions on oil palm leaf chromatin. The initial low DNA amounts generated ChIP-Seq data with low numbers of unique mapped reads at low coverage. This was even after pooling the DNA from six to eight ChIP reactions, which yielded between 1 and 10 ng DNA. It thus, appears that the number of ChIP reactions per sample will need to be scaled up significantly. ChIP yields obtained were lower than those obtained for maize, where a pool of three ChIP reactions yielded about 50 ng DNA (Oka *et al.*, 2017). As the purification of immunoprecipitated DNA is a necessary step before library preparation, assessing the efficiency of purification agents could help in maximising DNA recovery without compromising the quality. Among several commercial purification kits and reagents, DNA recovery was higher when phenol-chloroform was used (Zhong *et al.*, 2017).

Nevertheless, using targeted regions in analysing such imperfect datasets has been demonstrated to be a practical approach when a genome-wide interrogation is not feasible. This approach is in line with published ChIP-Seq guidelines when dealing with low-quality data validated based on several quantitative quality metrics (Landt *et al.*, 2012; Nakato and Shirahige, 2017). About 75% of the data could be mapped to a database comprising genes and their upstream and downstream regions, suggesting that these histone marks are enriched mostly at the genic areas of oil palm. Although read mapping to a smaller database does not always increase alignment sensitivity and specificity, it still holds several advantages. In practice, assigning reads to only selected biologically relevant positions could provide a quick estimate when addressing urgent biological problems, a QC step in a pilot study, or in any setting when focusing only on differentially expressed genes is justified. Besides, with large plant genome sizes rich with repeats, the use of a smaller functional database reduces the time for computational analysis and saves space for the storage of processing files. The different ChIP-Seq read coverage among biological replicates contributes to variation in numbers and regions of ChIP enrichment, thus, compromising reproducibility. However, enrichment of H3K4me3 and H3K27me3 marks near TSS is supported by the similar characteristics of these profiles in *Arabidopsis*, peach and potato (de la Fuente *et al.*, 2015; Yang *et al.*, 2018; Zeng *et al.*, 2019), indicating that the ChIP assay worked for oil palm even though sequence coverage was low. Scaling up the immunoprecipitation reactions or improving on the ChIP yield recovery would be required in future ChIP-Seq studies. In *Arabidopsis*, predicted enhancers were characterised and validated using open chromatin signatures, which include H3K27ac and H3K27me3 histone modification patterns and non-coding RNA with GUS-based reporter assays (Zhu *et al.*, 2015). Therefore, histone enrichment profiles could be used to verify predicted TSS locations and improve the annotation of the oil palm genome.

The number of sequencing reads needed to reach a reasonable coverage varies depending on the types of histone binding patterns of the various histone modification types. At least 20 million reads are required for sharp binding patterns, while 60 million reads are suggested for broad binding patterns (Landt *et al.*, 2012; Nakato and Shirahige, 2017). Read coverage is deemed sufficient when the saturation point could be established or when the same histone enrichment sites are repeatedly identified from additional sequencing. A way to improve read coverage is by evaluating the antibody's quality to capture histone-bound regions. The efficiency of the antibody can be tested by conducting a titration of chromatin experiment to a fixed amount of antibody. One can evaluate whether diluting chromatin would improve the precipitation efficiency, thus, assessing the

presence of inhibitory factors within the chromatin (Haring *et al.*, 2007). Monoclonal and polyclonal antibodies, which respectively recognise single and multiple epitopes, affect the degree of enrichment and background noise differently. Testing out several commercial antibodies is also advisable as different brands may exhibit different efficiencies. The number of individual ChIP reactions needs to be increased to achieve the required amount for library construction. However, low amounts of ChIP DNA may provide useful sequencing data if an appropriate sequencing library preparation method explicitly for low DNA input is used. Recently, as low as 0.01 ng DNA, which is ≥100x lower than the starting amount used in this study, can be used for constructing ChIP-sequencing libraries (reviewed by Dahl and Gilfillan, 2018). This is useful for single-cell analysis, whereby the ChIPmentation procedure offers a single-step reaction of chromatin fragmentation and adaptor tagging (Schmidl *et al.*, 2015). The reduction of library preparation steps compared to published ChIP-Seq protocols therefore allows for samples with low cell input, as yield losses throughout the procedure is also reduced. With emerging new technologies, the ChIP-Seq assay is now even feasible at the single-cell level (Clark *et al.*, 2016).

CONCLUSION

This is the first ChIP-Seq report on histone modification patterns for the oil palm *E. guineensis*. Although preliminary, the primary limitation in this study was the low coverage and high duplication of the H3K4me3 and H3K27me3 ChIP-Seq data due to low ChIP recovery. However, the data was still able to provide some preliminary insights on these histone profiles in oil palm through a gene-wide mapping approach, followed by peak calling. The traditional genome-wide mapping approach used for analysing ChIP-Seq data is not suitable for partially assembled genomes combined with the low read yield situation. Restriction to the functionally relevant areas in oil palm genome resulted in H3K4me3 and H3K27me3 profiles consistent with the profiles of these histone modifications in plants such as *Arabidopsis*, peach and potato. This study's findings and recommendations may be useful for other plant species with incomplete genome sequence information to accurately identify histone profiles without requiring intensive computational power.

ACKNOWLEDGEMENT

We are grateful to the Director-General of MPOB for permission to publish this study. We thank members of the Epigenetics Group, Advanced Biotechnology and Breeding Centre, MPOB for their invaluable technical support. We also thank Chan Kuang Lim and Nik Shazana Nik Sanusi from the Bioinformatics Unit, MPOB. Our appreciation also goes to the Clonal Propagation Group, MPOB for the clonal palms used in this study. This study was funded by the MPOB.

REFERENCES

Baulcombe, D C and Dean, C (2014). Epigenetic regulation in plant responses to the environment. *Cold Spring Harb. Perspect. Biol., 6*: 1-19.

Berenguer, E; Bárány, I; Solís, M-T; Pérez-Pérez, Y; Risueño, M C and Testillano, P S (2017). Inhibition of histone H3K9 methylation by BIX-01294 promotes stress-induced microspore totipotency and enhances embryogenesis initiation. *Front. Plant Sci., 8*: 1-19.

Chan, K-L; Tatarinova, T V; Rosli, R; Amiruddin, N; Azizi, N; Halim, M A A; Sanusi, N S N M; Jayanthi, N; Ponomarenko, P; Triska, M; Solovyev, V; Firdaus-Raih, M; Sambanthamurthi, R; Murphy, D and Low, E-T L (2017). Evidence-based gene models for structural and functional annotations of the oil palm genome. *Biol. Direct, 12(1)*: 21. DOI: 10.1186/s13062-017-0191-4.

Clark, S J; Lee, H J; Smallwood, S A; Kelsey, G and Reik, W (2016). Single-cell epigenomics: Powerful new methods for understanding gene regulation and cell identity. *Genome Biol., 17*: 1-10.

Dahl, J A and Gilfillan, G D (2018). How low can you go? Pushing the limits of low-input ChIP-seq. *Brief. Funct. Genomics, 17*: 89-95.

de la Fuente, L; Conesa, A; Lloret, A; Badenes, M L and Ríos, G (2015). Genome-wide changes in histone H3 lysine 27 trimethylation associated with bud dormancy release in peach. *Tree Genet. Genomes, 11*: 45. DOI: 10.1007/s11295-015-0869-7.

Dodt, M; Roehr, J T; Ahmed, R and Dieterich, C (2012). FLEXBAR-flexible barcode and adapter processing for next-generation sequencing platforms. *Biology (Basel), 1*: 895-905.

Engelhorn, J; Blanvillain, R; Kröner, C; Parrinello, H; Rohmer, M; Posé, D; Ott, F; Schmid, M and Carles, C (2017). Dynamics of H3K4me3 chromatin marks prevails over H3K27me3 for gene regulation during flower morphogenesis in *Arabidopsis thaliana. Epigenomes, 1*: 8. DOI: 10.3390/epigenomes1020008.

Gan, E-S; Xu, Y and Ito, T (2015). Dynamics of H3K27me3 methylation and demethylation in plant development. *Plant Signal. Behav., 10(9)*: e1027851.

Haring, M; Offermann, S; Danker, T; Horst, I; Peterhansel, C and Stam, M (2007). Chromatin immunoprecipitation: Optimization, quantitative analysis and data normalization. *Plant Methods, 3*: 11. DOI: 10.1186/1746-4811-3-11.

Kaufmann, K; Muiño, J M; Østerås, M; Farinelli, L; Krajewski, P and Angenent, G C (2010). Chromatin immunoprecipitation (ChIP) of plant transcription factors followed by sequencing (ChIP-SEQ) or hybridization to whole genome arrays (ChIP-CHIP). *Nat. Protoc., 5(3)*: 457-472.

Landt, S G; Marinov, G K; Kundaje, A; Kheradpour, P; Pauli, F; Batzoglou, S; Bernstein, B E; Bickel, P; Brown, J B; Cayting, P; Chen, Y; DeSalvo, G; Epstein, C; Fisher-Aylor, K I; Euskirchen, G; Gerstein, M; Gertz, J; Hartemink, A J; Hoffman, M M; Iyer, V R; Jung, Y L; Karmakar, S; Kellis, M; Kharchenko, P V; Li, Q; Liu, T; Liu, S; Ma, L; Milosavljevic, A; Myers, R M; Park, P J; Pazin, M J; Perry, M D; Raha, D; Reddy, T E; Rozowsky, J; Shoresh, N; Sidow, A; Slattery, M; Stamatoyannopoulos, J A; Tolstorukov, M Y; White, K P; Xi, S; Farnham, P J; Lieb, J D; Wold, B J and Snyder, M (2012). ChIP-seq guidelines and practices of the ENCODE and modENCODE consortia. *Genome Res., 22*: 1813-1831.

Langmead, B and Salzberg, S L (2012). Fast gapped-read alignment with Bowtie2. *Nat. Methods, 9*: 357-359.

Li, H; Handsaker, B; Wysoker, A; Fennell, T; Ruan, J; Homer, N; Marth, G; Abecasis, G and Durbin, R (2009). The sequence alignment/map format and SAMtools. *Bioinformatics, 25*: 2078-2079.

Liu, E T; Pott, S and Huss, M (2010). Q&A: ChIP-seq technologies and the study of gene regulation. *BMC Biol., 8*: 56. DOI: 10.1186/1741-7007-8-56.

Loh, Y-H E; Feng, J; Nestler, E and Shen, L (2017). Bioinformatic analysis for profiling drug-induced chromatin modification landscapes in mouse brain using ChIP-seq data. *Bio Protoc., 7(3)*: e2123. DOI: 10.21769/BioProtoc.2123.

Lu, Y; Zhou, D-X and Zhao, Y (2020). Understanding epigenomics based on the rice model. *Theor. Appl. Genet., 133*: 1345-1363.

Nakato, R and Shirahige, K (2017). Recent advances in ChIP-seq analysis: From quality management to whole-genome annotation. *Brief. Bioinform., 18*: 279-290.

Oka, R; Zicola, J; Weber, B; Anderson, S N; Hodgman, C; Gent, J I; Wesselink, J-J; Springer, N M; Hoefsloot, H C J; Turck, F and Stam, M (2017). Genome-wide mapping of transcriptional enhancer candidates using DNA and chromatin features in maize. *Genome Biol., 18(1)*: 137. DOI: 10.1186/s13059-017-1273-4.

Ong-Abdullah, M; Ordway, J M; Jiang, N; Ooi, S-E; Kok, S-Y; Sarpan, N; Azimi, N; Hashim, A T; Ishak, Z; Rosli, S K; Malike, F A; Bakar, N A A; Marjuni, M; Abdullah, N; Yaakub, Z; Amiruddin, M D; Nookiah, R; Singh, R; Low, E-T L; Chan, K-L; Azizi, N; Smith, S W; Bacher, B; Budiman, M A; Van Brunt, A; Wischmeyer, C; Beil, M; Hogan, M; Lakey, N; Lim, C-C; Arulandoo, X; Wong, C-K; Choo, C-N; Wong, W-C; Kwan, Y-Y; Alwee, S S R S; Sambanthamurthi, R and Martienssen, R A (2015). Loss of Karma transposon methylation underlies the mantled somaclonal variant of oil palm. *Nature, 525*: 533-537.

Ong-Abdullah, M; Ordway, J M; Jiang, N; Ooi, S-E; Mokri, A; Kok, S Y; Sarpan, N; Azimi, N; Hashim, A T; Ishak, Z; Rosli, S K; Nookiah, R; Singh, R; Low, E-T L; Sachdeva, M; Smith, S W; Lakey, N; Martienssen, R A and Sambanthamurthi, R (2016). Tissue culture and epigenetics. *The Planter, 92*: 741-749.

Prakash, K and Fournier, D (2018). Evidence for the implication of the histone code in building the genome structure. *Biosystems, 164*: 49-59.

Ranawaka, B; Tanurdzic, M; Waterhouse, P and Naim, F (2020). An optimised chromatin immunoprecipitation (ChIP) method for starchy leaves of *Nicotiana benthamiana* to study histone modifications of an allotetraploid plant. *Mol. Biol. Rep., 47*: 9499-9509.

Sanusi, N S N M; Rosli, R; Halim, M A A; Chan, K-L; Nagappan, J; Azizi, N; Amiruddin, N; Tatarinova, T V and Low, E-T L (2018). PalmXplore: Oil palm gene database. *Database, 2018*: 1-9.

Sarpan, N; Ong-Abdullah, M and Ooi, S-E (2018). Optimisation of a chromatin immunoprecipitation (ChIP) protocol for histone modification in oil palm. *J. Oil Palm Res., 30*: 242-250.

Schmidl, C; Rendeiro, A F; Sheffield, N C and Bock, C (2015). ChIPmentation: Fast, robust, low-input ChIP-seq for histones and transcription factors. *Nat. Methods, 12*: 963-965.

Shahmuradov, I A; Umarov, R K and Solovyev, V V (2017). TSSPlant: A new tool for prediction of plant Pol II promoters. *Nucleic Acids Res., 45(8)*: e65.

Singh, R; Ong-Abdullah, M; Low, E-T L; Manaf, M A A; Rosli, R; Nookiah, R; Ooi, L C-L; Ooi, S-E; Chan,

K-L; Halim, M A; Azizi, N; Nagappan, N; Bacher, B; Lakey, N; Smith, S W; He, D; Hogan, M; Budiman, M A; Lee, E K; DeSalle, R; Kudrna, D; Goicoechea, J L; Wing, R A; Wilson, R K; Fulton, R S; Ordway, J M, Martienssen, R A and Sambanthamurthi, R (2013). Oil palm genome sequence reveals divergence of interfertile species in old and new worlds. *Nature, 500*: 335-339.

Wollmann, H and Berger, F (2012). Epigenetic reprogramming during plant reproduction and seed development. *Curr. Opin. Plant Biol., 15*: 63-69.

Yang, Z; Qian, S; Scheid, R N; Lu, L; Chen, X; Du, X; Lv, X; Boersma, M D; Scalf, M and Smith, L M (2018). EBS is a bivalent histone reader that regulates floral phase transition in *Arabidopsis. Nat. Genet., 50*: 1247-1253.

Zeng, Z; Zhang, W; Marand, A P; Zhu, B; Buell, C R and Jiang, J (2019). Cold stress induces enhanced chromatin accessibility and bivalent histone modifications H3K4me3 and H3K27me3 of active genes in potato. *Genome Biol., 20*: 1-17.

Zhang, W; Garcia, N; Feng, Y; Zhao, H and Messing, J (2015). Genome-wide histone acetylation correlates with active transcription in maize. *Genomics, 106(4)*: 214-220.

Zhang, X; Bernatavichute, Y V; Cokus, S; Pellegrini, M and Jacobsen, S E (2009). Genome-wide analysis of mono-, di- and trimethylation of histone H3 lysine 4 in *Arabidopsis thaliana. Genome Biol., 10(6)*: R62. DOI: 10.1186/gb-2009-10-6-r62.

Zhang, Y; Liu, T; Meyer, C A; Eeckhoute, J; Johnson, D S; Bernstein, B E; Nussbaum, C; Myers, R M; Brown, M; Li, W and Liu, X S (2008). Model-based analysis of ChIP-Seq (MACS). *Genome Biol., 9(9)*: R137. DOI: 10.1186/gb-2008-9-9-r137.

Zhong, J; Ye, Z; Lenz, S W; Clark, C R; Bharucha, A; Farrugia, G; Robertson, K D; Zhang, Z; Ordog, T and Lee, J-H (2017). Purification of nanogram-range immunoprecipitated DNA in ChIP-seq application. *BMC Genomics, 18(1)*: 985. DOI: 10.1186/s12864-017-4371-5.

Zhu, B; Zhang, W; Zhang, T; Liu, B and Jiang, J (2015). Genome-wide prediction and validation of intergenic enhancers in *Arabidopsis* using open chromatin signatures. *Plant Cell, 27*: 2415-2426.

Zong, W; Zhong, X; You, J and Xiong, L (2013). Genome-wide profiling of histone H3K4-tri-methylation and gene expression in rice under drought stress. *Plant Mol. Biol., 81*: 175-188.

Zulkifli, Y; Norziha, A; Naqiuddin, M H; Fadila, A M; Nor Azwani, A B; Suzana, M; Samsul, K R; Ong-Abdullah, M; Singh, R; Parveez, G K A and Kushairi, A (2017). Designing the oil palm of the future. *J. Oil Palm Res., 29*: 440-455.